

SUPPLEMENTARY METHODS

Generation of induced pluripotent stem cells

Human induced pluripotent stem cell line HPSI1113i-wetu_2 used as a control line was kindly provided by the Wellcome Trust Sanger Institute, UK. Generation of iPSCs from patients was performed using the CytoTune[®]-iPS 2.0 Sendai Reprogramming Kit. In brief, 2×10^5 cells/cm² were transduced with the non-transmissible Sendai virus harbouring the genetic factors SOX2, KLF4, OCT4 and c-MYC in the presence of 10 µg/ml Polybrene. Subsequently, the cells were cultured in StemPro[®]-34SFM medium supplemented with StemPro[®]-34 Nutrient Supplement, 2 mM glutamine, 100 ng/ml stem cell factor, 100 ng/ml fms-like tyrosine kinase 3, 20 ng/ml interleukin-3, 20 ng/ml interleukin-6 and 2 U/ml erythropoietin. After two days, the transduced cells were transferred onto Matrigel-coated plates and the medium was successively switched from StemPro[®]-34SFM medium supplemented with StemPro[®]-34 Nutrient Supplement and 2 mM glutamine to Essential 7 (E7) medium (DMEM/F12, 64 µg/ml L-ascorbic acid 2-phosphate, 20 µg/ml insulin, 5 µg/ml transferrin, 14 ng/ml sodium selenite, 100 ng/ml fibroblast growth factor 2), and finally to Essential 8 (E8) medium (E7 medium with 2 ng/ml transforming growth factor β1). Ultimately, the cells were cultured in E8 medium. Undifferentiated colonies were picked and cultured in E8 supplemented with 10 µg/ml Y27632.

For experimentation, all iPSC lines were cultured on Matrigel-coated culture dishes in Essential 8 medium. The culture medium was changed daily. Cells were recovered and passaged at a density of 70 – 80% using accutase or 0.5M EDTA/DPBS. For SNP karyotyping, iPSC pellets were resuspended in 200 µl of PBS and genomic DNA was isolated using the DNeasy blood and tissue kit (Qiagen, Valencia, CA). DNA samples were SNP karyotyped using the Infinium OmniExpressExome-8 Kit and the iScan system from Illumina. CNV and SNP visualization were performed using KaryoStudio v1.4 (Illumina).

Sequencing

To verify the presence of the *LRP2* mutation in patient-derived iPSC lines, primers were generated using the DNASTar Seqbuilder Software Version 13.0.0 that flank the mutation at position c:G9575A. Primer sequences were as follows:

LRP2fw: AAGCTCATGTCTGACAAGCGGACT,

LRP2rev: TACAATCTCTTCTCTACTCGGTC.

The Phire Animal Tissue Direct PCR kit (Thermo Fisher Scientific) was used to amplify a genomic DNA fragment containing the *LRP2* mutation. The PCR products were purified using the ExoSAP-ITTM PCR Product Cleanup reagent (Thermo Fisher Scientific). DNA sequencing was performed by LGC Genomics GmbH (Germany) and data analysed using the DNASTar SeqMan Software Version 13.0.0.

***LRP2* gene disruption in iPSCs**

The deletion of *LRP2* gene in human iPSC line HPSI1113i-wetu_2 was achieved by using the CRISPR/Cas9 system. Single guide RNA (sgRNA) targeting the start codon of *LRP2* gene was designed using the online software tool provided by Zhang lab (crispr.mit.edu). sgRNA sequences were as follows: sense: CCGTCGCGGAGATGGATCGC and antisense: GCGATCCATCTCCGCGACGG. Annealed sgRNA oligonucleotides were cloned into the expression vector pSpCas9(BB)-2A-GFP (PX458, Addgene plasmid #48138) following digesting with FastDigest BbsI (Thermo Fisher Scientific). Human iPSCs were transfected with the final sgRNA-plasmid construct using Lipofectamine3000 (Thermo Fisher Scientific) according to manufacturer's protocol. Transfected cells were selected with 0.1 µg/ml puromycin for one week before seeding them at low density for single cell colony expansion. Clones were analyzed for successful deletion using the Phire Animal Tissue Direct PCR kit. Primer sequences used were: LRP2KOfw: AGGGCTTTATGCACTGTCTGG; LRP2KOrev: AGGCTCTGGCTGGGCTCTT. DNA sequencing to confirm genome editing was performed

by LGC Genomics GmbH and data analyzed using the DNASTar SeqMan Software Version 13.0.0.

Differentiation of iPSCs to NPCs

The neuroectodermal differentiation protocol was adapted from a published protocol ¹. In detail, iPSCs were dissociated with accutase to single cell suspension and 20.000 cells/cm² plated on Matrigel-coated dishes in E8 medium supplemented with 10 µg/ml of Rock inhibitor Y27632. Cells were allowed to grow for 3 days until they were nearly confluent, after which the medium was changed to N2B27 differentiation medium containing 100 ng/ml noggin, 200 nM dorsomorphin (inhibitor of the bone morphogenetic/activin pathway) and 10 µM SB431542 (inhibitor of transforming growth factor β/activin pathway). Medium change was performed daily. At day 5, the medium was replaced by N2B27 containing noggin, dorsomorphin, and 200 ng/ml sonic hedgehog, and cells were grown for up to 4 more days. For rosette formation, cells were re-plated at day 5 at high density (1:2) on Matrigel-coated plates and fixed at day 7 for immunocytochemistry.

Differentiation of iPSC to RPTECs

The differentiation protocol was adapted from ². Briefly, iPSCs were dissociated into single cells using accutase and 10.000 cells/cm² were plated on Matrigel-coated dishes in E8 medium supplemented with 10 µg/ml Rock inhibitor Y27632. When cells reached 75-80% confluence depicted as day 0 of differentiation, medium was changed to STEMdiff™ APEL™ 2 medium (Stem Cell Technologies) supplemented with 10 ng/ml Activin A, 30 ng/ml BMP4 and 1 µM retinoic acid to induce mesodermal fate. At day 4, medium was changed to APEL supplemented with 150 ng/ml GDNF to induce renal vesicle differentiation. Upon differentiation day 8, renal epithelial growth medium (REGM, Lonza) was utilized for

tubular epithelial specification. During the course of differentiation, medium was replaced every other day.

Fluorescence immunocytochemistry

Cells were fixed in 4% paraformaldehyde for 10 minutes at room temperature, washed with PBS, blocked and permeabilised in PBS containing 0.2% gelatine, 0.1% saponin and 5 mg/ml BSA for 10 minutes. Primary antibodies were diluted in washing solution (PBS containing 0.2% gelatine and 0.01% saponin) and cells incubated over night at 4°C. Then, the cells were washed with washing solution and incubated with the secondary antibodies coupled to Alexa fluorophores for 1 hour at room temperature. Cells were mounted in Prolong Diamond Antifade Mountant containing DAPI (Thermo Fisher Scientific). Antibodies used were directed against OCT4 (Abcam, ab19857; 1:100), SOX2 (Abcam, ab97959; 1:100), Nanog (R&D, 1:100), SSEA4 (Abcam, ab16287; 1:100), megalin (produced in-house; 1:250), LAMP1 (Cell Signaling, 9091P; 1:700), GST (Cell Signaling, 624S; 1:100), PAX6 (BioLegend, 9019301; 1:100), SOX1 (Abcam, ab109290; 1:100), and AQP1 (Proteintech, 20333-1-AP, 1:100). For assessing germ layer differentiation, the human germ layer 3-Color Immunocytochemistry kit (R&D) was used.

Ligand treatment

For analysis of ligand impact on megalin activity, cells were starved in blank medium for 2 hours before addition of 10 µg/ml GST-SHH-N or GST, or 20 µg/ml lysozyme in DMEM/1.5% BSA. After ligand incubation for the time points indicated in the respective figure legends, cells were either fixed in 4% paraformaldehyde for immunofluorescence analysis or lysed for western blotting. Antibodies used for Western blotting were goat anti-rabbit megalin (produced in-house; 1:500), anti-GST (Cell Signaling; 624S, 1:1000), anti-lysozyme (Abcam, ab391, 1:500), and anti-tubulin (Calbiochem; CP06, 1:1000).

Cycloheximide experiments

To determine megalin stability, replicate layers of cells were treated with 10 µg/ml GST-SHH-N and 7.5 µg/ml cycloheximide in N2B27 medium from day 5 of neuroectodermal differentiation onwards. During incubation time, the cell culture medium with freshly added ligand and cycloheximide was changed daily. Cells were lysed for analysis of megalin levels by western blotting at the indicated time points.

Lysosomal inhibition

Replicate cell layers were differentiated into NPCs until day 5. Activity of lysosomal proteases was blocked by adding a cocktail of 100 µM leupeptin, 10 µM pepstatin and 50 µM chloroquine for 1 hour. Afterwards, cells were incubated with 10 µg/ml GST-SHH-N and lysosomal inhibitors overnight before analyzing megalin levels by western blotting.

SUPPLEMENTARY REFERENCES

1. Chambers SM, Fasano CA, Papapetrou EP, *et al.* Highly efficient neural conversion of human ES and iPS cells by dual inhibition of SMAD signaling. *Nat Biotechnol* 2009; **27**: 275-280.
2. Hariharan K, Stachelscheid H, Rossbach B, *et al.* Parallel generation of easily selectable multiple nephronal cell types from human pluripotent stem cells. *Cell Mol Life Sci* 2019; **76**: 179-192.

SUPPLEMENTARY FIGURE LEGENDS

Figure S1: Karyotypes of iPSC lines from patients with Donnai-Barrow syndrome

(A, B) Chromosome 2 ideogram from peripheral blood mononuclear cells (PBMC) of patients R3192Q_1 (A) and R3192Q_2 (B). The logR ratio (red data points) depicts single nucleotide polymorphism intensity signals indicative of potential duplications or deletions in this chromosome locus. The B allele frequency (blue data point) gives the relative frequency of one allele compared to the other. Both patients are characterized by CN-LOH at 2q23.3-q31.1 encompassing *LRP2*. **(C, D)** Virtual karyotypes of PBMC and iPSC from patients R3192Q_1 (C) and R3192Q_2 (D). Insertions (green), deletions (red), and regions with copy neutral loss of heterozygosity (CN-LOH; grey) are indicated.

Figure S2: Pluripotency markers and differentiation potential of iPSCs from Donnai-Barrow patients

(A) Bright field images and immunocytochemical detection of pluripotency markers OCT4 (red), SOX2 (red), NANOG (red), and SSEA4 (green) in iPSCs from patients R3192Q_1 and R3192Q_2 compared to control cells. Cells were counterstained with DAPI (blue). Scale bars: 100 μm (bright field) or 25 μm (immunostainings). **(B)** Quantitative (q) RT-PCR analysis of the indicated pluripotency markers in patient and control iPSCs. Data are depicted as ct values normalized to transcript levels of *GAPDH* ($\Delta\text{ct} \pm \text{SD}$) as internal control. This experiment was performed in 3 independent biological replicates. No statistically significant differences in transcript levels of these pluripotency markers were seen comparing cell lines (Student's *t*-test). **(C)** iPSCs were differentiated into the three germ layers and differentiation assessed by immunocytochemical detection of ectoderm marker OTX2 (red) and SOX2 (red), endoderm marker GATA4 (green) and SOX17 (red), as well as mesoderm marker HAND1 (red). Cells were counterstained with DAPI (blue). Scale bar: 10 μm . **(D)** qRT-PCR analysis of the

indicated markers in differentiated patient and control cells as exemplified in (C). Data are depicted as ct values normalized to internal *GAPDH* transcript levels ($\Delta\text{ct} \pm \text{SD}$). This experiment was performed in 3 independent biological replicates. No statistically significant differences in transcript levels of these marker genes were seen comparing cell lines (Student's *t*-test).

Figure S3: Neuroectodermal differentiation of iPSC lines from Donnai-Barrow patients

(A) Protocol for neuroectodermal differentiation of iPSCs to neural progenitor cells (NPCs).

The protocol used was adapted from ¹ (see supplementary methods for details). **(B, C)**

Immunocytochemical detection of early neuroectodermal markers PAX6 (green; B) and SOX1 (green; C) in iPSC lines from patients R3192Q_1 and R3192Q_2 as compared to control cells at day 2, 5, and 9 of differentiation. Cells were counterstained with DAPI (blue). Scale bar: 25 μm .

(D, E) Quantitative RT-PCR analysis of the pluripotency marker *OCT4* and early neuroectodermal marker *PAX6* in iPSCs from patients R3192Q_1 (D) and R3192Q_2 (E) as compared to control cells at day 2, 5, and 9 of differentiation. Data are depicted as Δct values normalized to the mean of the control cells at day 0 ($\Delta\Delta\text{ct}$) \pm SD (n=1-4 experiments with 2-3 biological replicates/experiment). Statistical analysis was determined by Two-way Anova. No statistically significant differences were found using Bonferroni post-test comparing genotypes at the given time points.

Figure S4: Megalin^{R3192Q} expression is impaired post-transcriptionally in a second patient

(A) Immunodetection of megalin (red) in iPSCs from control and Donnai-Barrow patient R3192Q_2 at the indicated time points of neuroectodermal differentiation. Cells were counterstained with DAPI (blue). Megalin expression is induced from day 5 onwards in both genotypes. At day 9, megalin levels are decreased in patient-derived NPCs as compared to

control cells. Scale bar: 10 μ m. **(B)** Transcript levels of *LRP2* during differentiation were analyzed in iPSCs from a control subject and patient R3192Q_2. Data are depicted as Δ ct normalized to day 0 of the control cells ($\Delta\Delta$ ct) \pm SD (n=1 experiment with 2 biological replicates per genotype). Statistical analysis was performed by Two-way Anova with a Bonferroni post-test. **, p<0.01 **(C)** Representative western blot analysis of megalin levels in control and R3192Q_2 iPSC lines at the indicated time points of differentiation. Detection of tubulin served as loading control. **(D)** Megalin levels were quantified by densitometric scanning of replicate western blots (as exemplified in panel C) in control and R3192Q_2 NPCs at day 5 and at day 9 of neuronal differentiation (n=3 independent experiments with 3 biological replicates/experiment). Values are given as relative levels of expression compared to control (set to 100% \pm SD). Megalin levels in R3192Q_2 cells are comparable to control cells at day 5, but significantly decreased at day 9 of differentiation. Statistical significance was determined by Student's *t*-test. ****, p<0.0001. **(E)** Quantitative RT-PCR analysis of *LRP2* transcript levels in control and R3192Q_2 NPCs cells at day 5 and 9 of differentiation. (n=3 independent experiments with 3 biological replicates/experiment). Levels are depicted as ct values normalized to transcript levels of *GAPDH* (Δ ct \pm SD) used as internal control. Transcript levels for *LRP2* are unchanged comparing the two genotypes as determined by Student's *t*-test.

Figure S5: Generation of iPSCs genetically deficient for *LRP2*

(A) Sequence analysis showing homozygosity for a 13 nucleotides deletion including the ATG start codon (highlighted in blue) in a *LRP2*^{-/-} cell clone derived from the parental control cell line (*LRP2*^{+/+}) by CRISPR/Cas9-mediated genome editing (see supplementary methods for details). Sequences for cell lines *LRP2*^{-/-} and *LRP2*^{+/+} were aligned to the *LRP2* reference sequence given above (NCBI Reference Sequence: NM_004525.2). **(B)** NPCs from cell lines *LRP2*^{-/-} and *LRP2*^{+/+} at day 9 of differentiation were treated overnight in medium containing

10 µg/ml recombinant GST-SHH-N. Thereafter, levels of megalin and GST-SHH-N in cell lysates were analyzed by western blotting. Two biological replicates are shown for each cell line. Detection of tubulin served as loading control. Expression of megalin is readily detected in control cells but absent from the receptor null clone *LRP2*^{-/-}. (C) NPCs from cell lines *LRP2*^{-/-} and *LRP2*^{+/+} at day 7 of differentiation were treated for 2 h in medium containing 10 µg/ml recombinant GST-SHH-N. Subsequently, the cells were immunostained for GST-SHH-N (red) using anti-GST antisera and counterstained with DAPI (blue). Scale bar: 25 µm. (D) Uptake of GST-SHH-N in NPCs from cell lines *LRP2*^{-/-} and *LRP2*^{+/+} at day 9 of differentiation was quantified by densitometric scanning of replicate western blots (as exemplified in panel B). Levels are given relative to control cells (set to 100% ± SD). The amount of internalized GST-SHH-N is significantly lower in *LRP2*^{-/-} cells as compared to control cells (n= 2 independent exemplary experiments, 1-2 biological replicates/experiment; Student's *t*-test). **, p<0.01.

Figure S6: Ligand-induced decay of megalin^{R3192Q} in NPCs from a second patient

(A) NPCs at day 5 of differentiation were treated with 10 µg/ml GST-SHH-N or blank medium overnight and levels of megalin were determined in cell lysates thereafter. Detection of α-tubulin served as loading control. (B) Quantification of megalin levels in control and R3192Q_2 NPC lines by densitometric scanning of replicate western blots (as exemplified in panel A). Levels are given as relative to the untreated condition (set at 100% ± SD). In the presence of GST-SHH-N, levels of megalin^{R3192Q} were significantly lower compared to that of the wild-type receptor (n= 4 independent experiments, 2-3 biological replicates/experiment). This difference was not seen in control medium (blank) lacking the receptor ligand. Statistical significance was determined using Student's *t*-test. *, p<0.05.

Figure S7: Differentiation of iPSCs into renal proximal tubular epithelial-like cells

(A) Protocol for differentiation of iPSCs into renal proximal tubular epithelial-like cells (RPTECs). The protocol was adapted from ². (B) Quantitative RT-PCR analysis of mesodermal marker *T/Brachyury*, renal vesicle marker *JAG1*, proximal tubule marker *AQP1*, and *LRP2* in iPSCs from R3192Q_1 as compared to control cells at day 4, 8, 10, 12 and 14 of differentiation. Data are depicted as $\Delta\Delta\text{ct}$ values normalized to control cells at day 0 ($\Delta\Delta\text{ct} \pm \text{SD}$; n=3 experiments). Statistical analysis was performed by Two-way Anova with Bonferroni post-test. No statistically significant differences in gene transcript levels were seen comparing genotypes. (C) Immunofluorescence detection of aquaporin-1 (AQP1, green) and megalin (red) in control and R3192Q_1 cells at day 10 of differentiation. Cells were counterstained with DAPI (blue). Scale bar: 10 μm .

Figure S8: Lysozyme does not induced decay of megalin^{R3192Q} in RPTECs

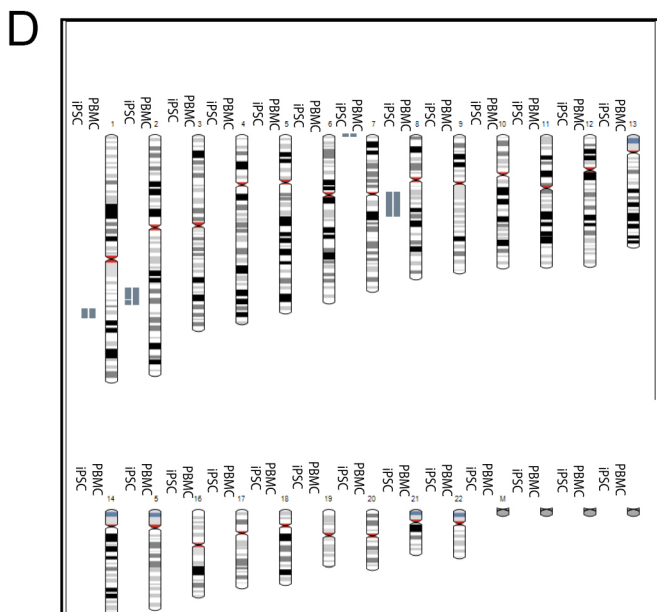
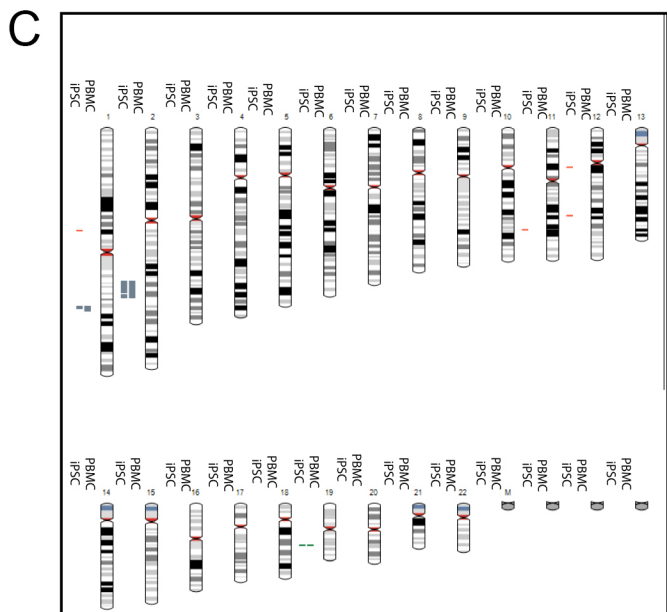
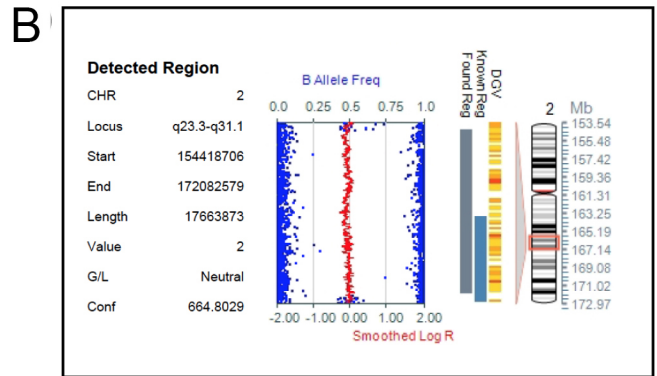
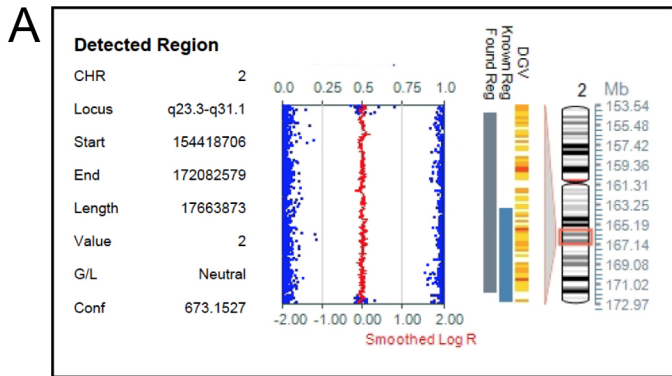
(A) Control and iPSC-derived RPTECs at differentiation day 8 were treated with 20 $\mu\text{g/ml}$ lysozyme or with blank medium overnight. Subsequently, megalin levels were determined by western blotting of cell lysates. Detection of α -tubulin served as loading control. (B) Megalin levels in control and R3192Q_1 were quantified by densitometric scanning of replicate western blots (exemplified in panel A). Levels are given as relative to the untreated condition (set at 100% \pm SD). No statistical significance of data was seen with blank or lysozyme-treatment condition comparing the two genotypes (n=3 independent experiments, 2-3 biological replicates/experiment; Student's *t*-test).

Figure S9: Binding of GST-SHH-N directs megalin^{R3192Q} to lysosomes in NPCs from a second patient

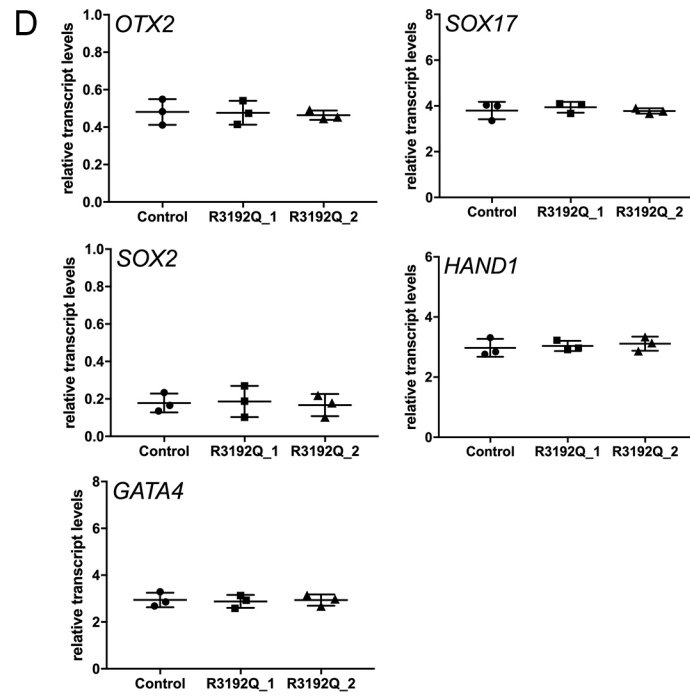
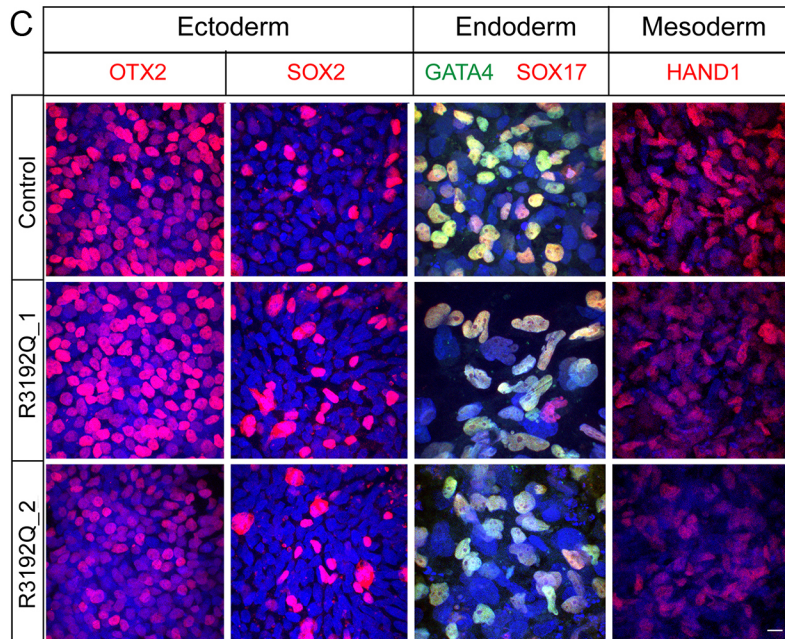
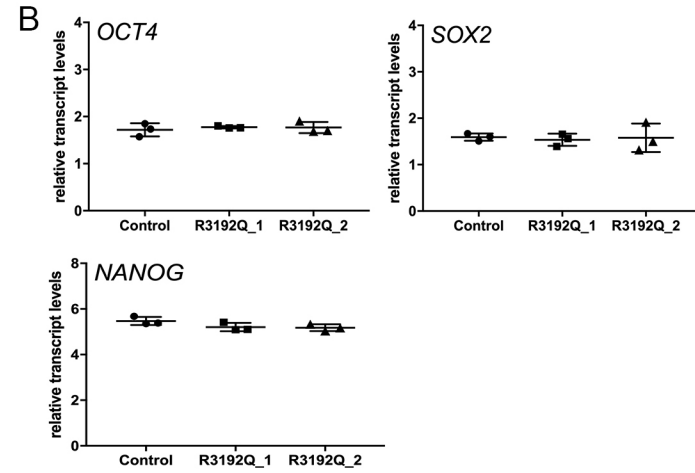
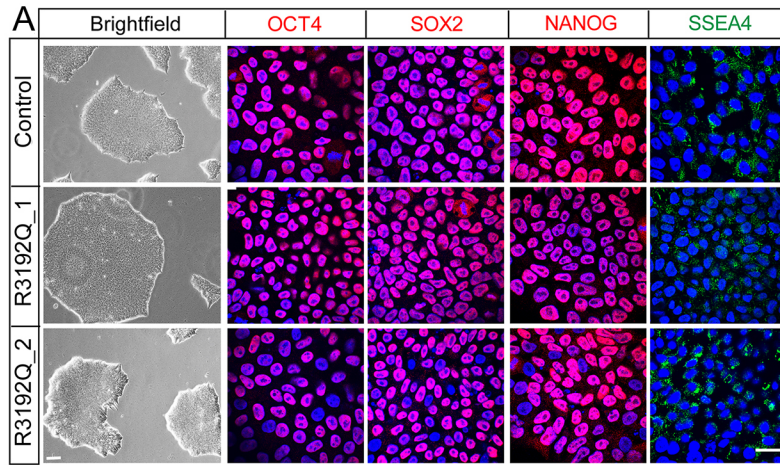
(A) Immunofluorescence detection of megalin (red) and GST-SHH-N (green) in control and patient NPCs at day 7 of differentiation. Cells were treated with 10 $\mu\text{g/ml}$ GST-SHH-N for 2

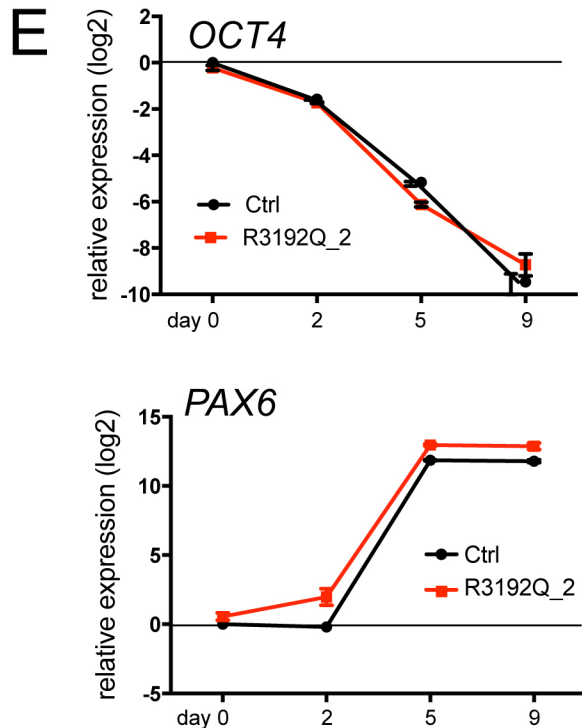
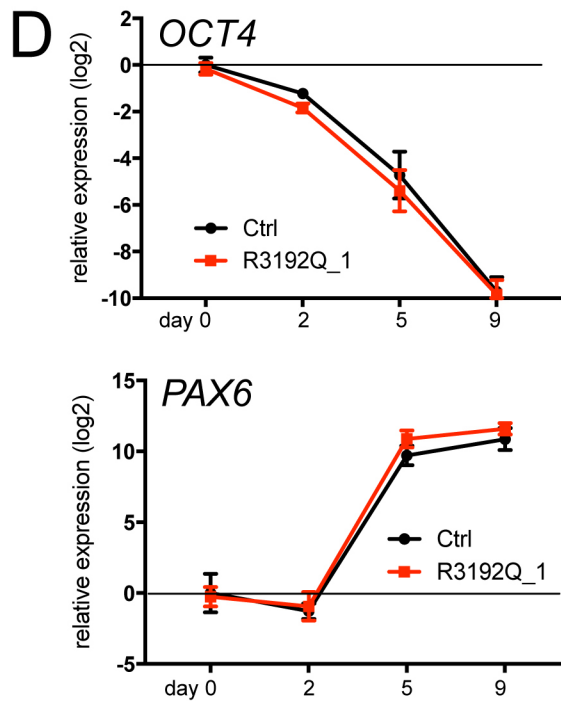
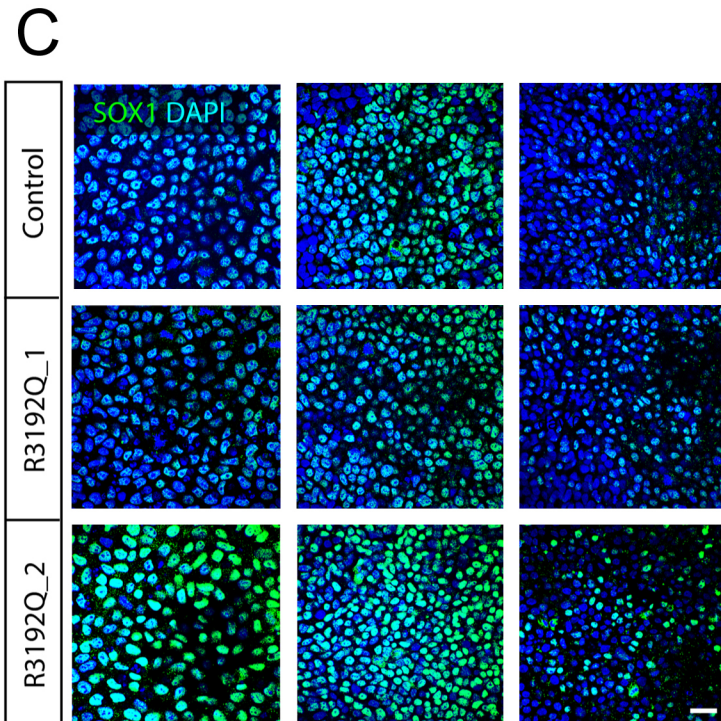
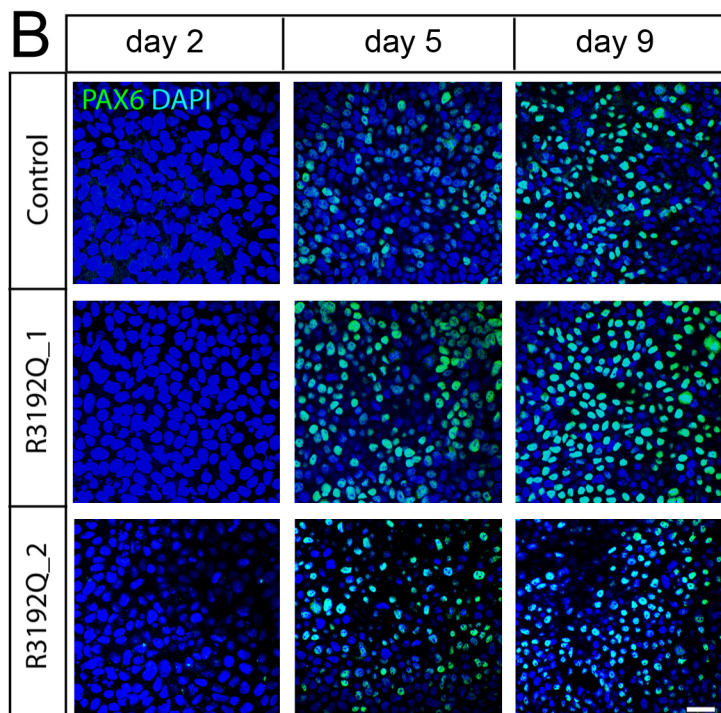
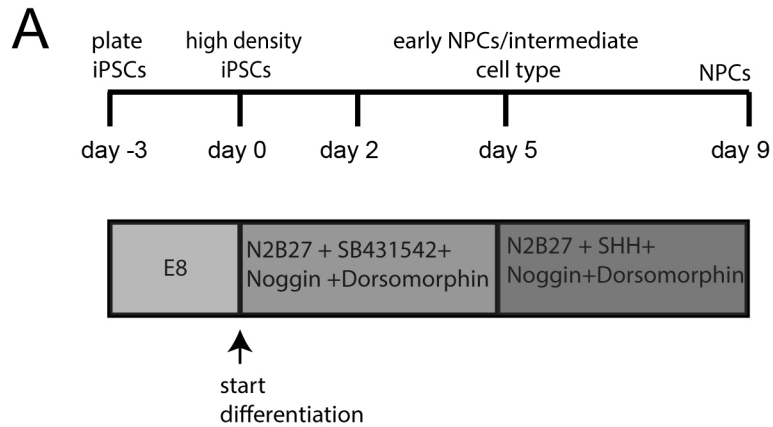
hours. Scale bar: 8 μm . **(B)** Co-localization of megalin with GST-SHH-N as determined by Mander's co-localization coefficient is increased for megalin^{R3192Q} as compared to wild-type megalin, suggesting prolonged interaction of the mutant receptor with ligands. One representative experiment is shown with data given as mean \pm SD. This experiment was repeated 4 times with 25-40 cells/experiment analyzed. Two experiments showed statistical significance and one experiment a clear trend (Student's *t* test). *, $p < 0.05$. **(C)**

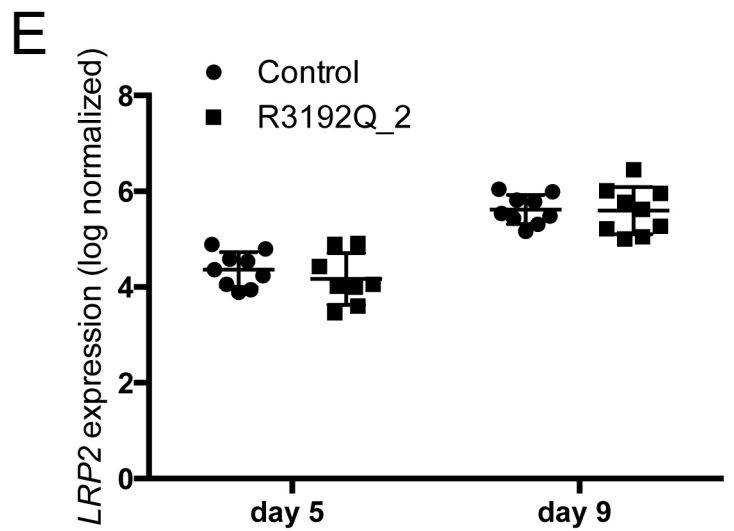
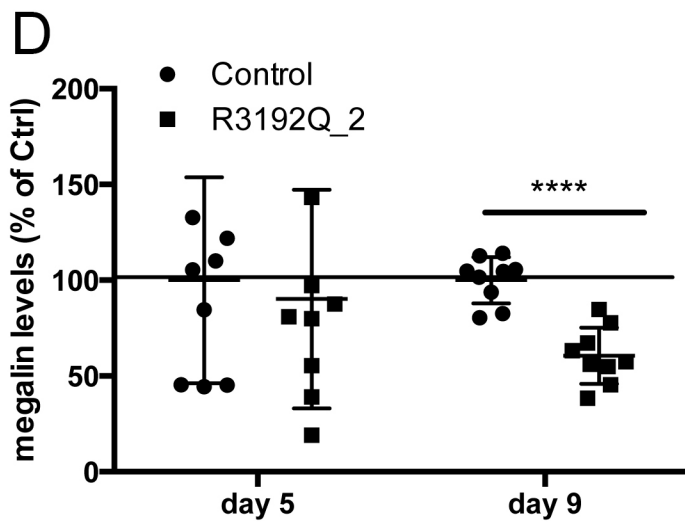
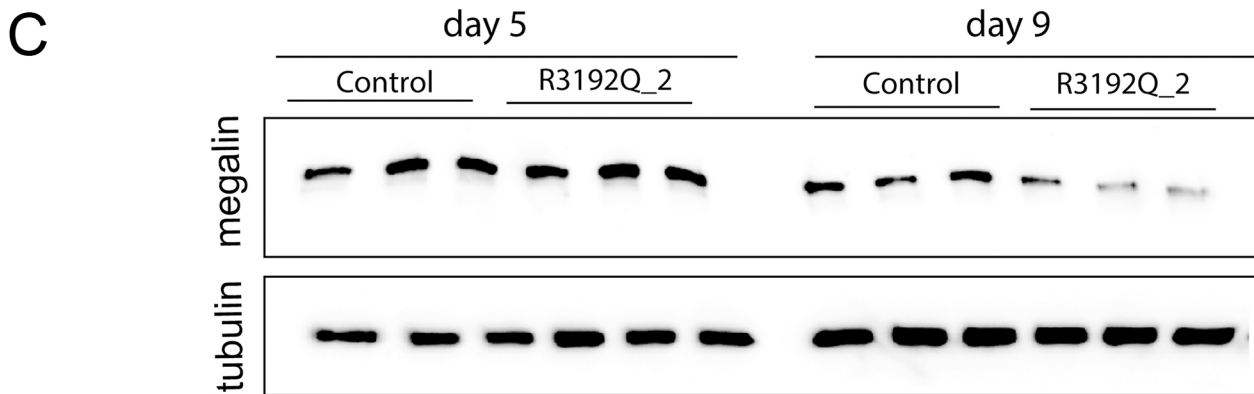
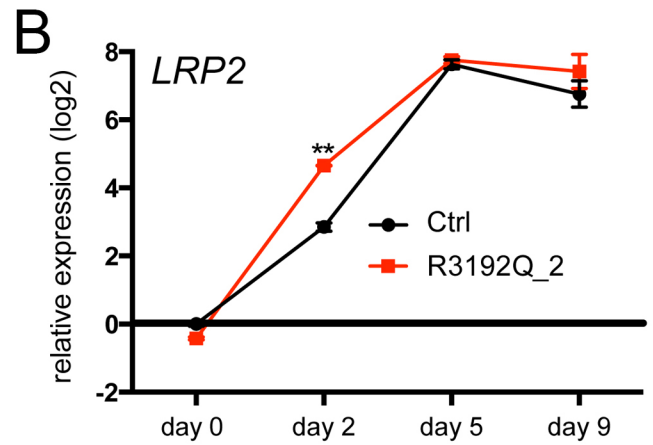
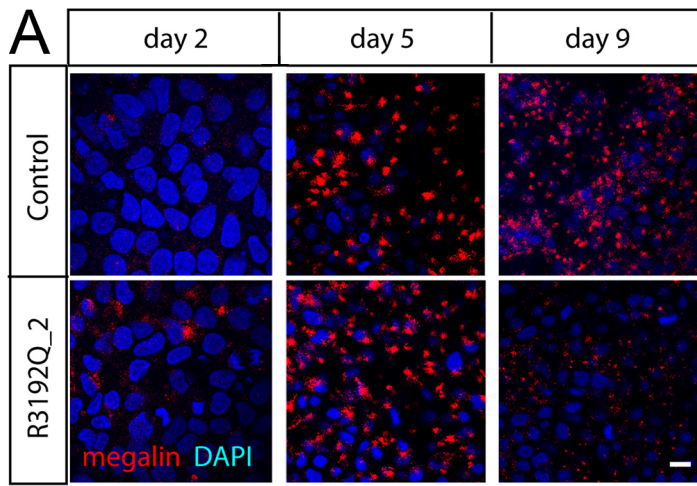
Immunofluorescence detection of megalin (red) and lysosomal marker LAMP1 (green) in control and patient NPC at day 7 of differentiation. Cells were treated with 10 $\mu\text{g/ml}$ GST or GST-SHH-N for 2 hours. Scale bar: 8 μm . **(D)** Mander's co-localization coefficient documents increased co-localization of megalin^{R3192Q} with LAMP1 in NPC treated with GST-SHH-N as compared to wild-type megalin (n=mean of 4 experiments with 10-40 cells/experiment analyzed \pm SD; Student's *t* test). **, $p < 0.01$.

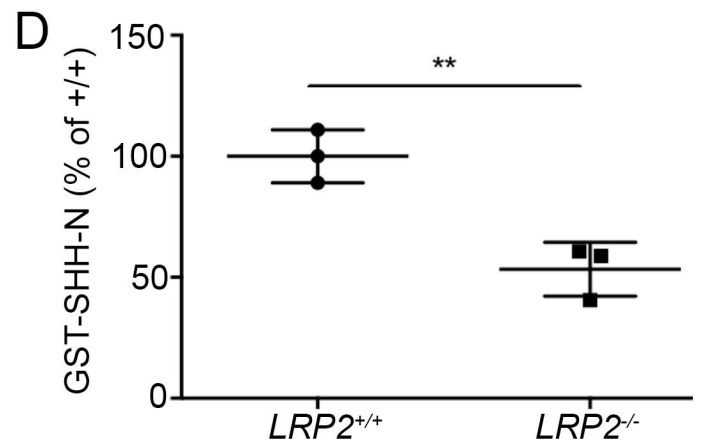
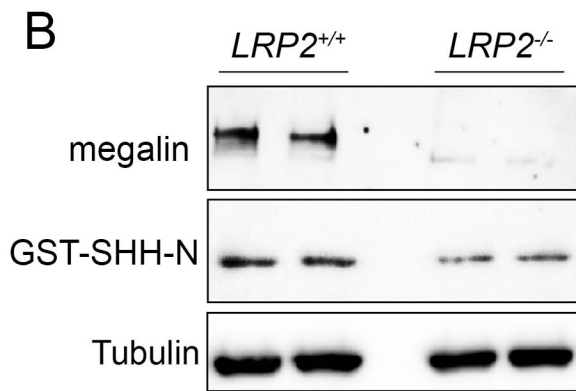
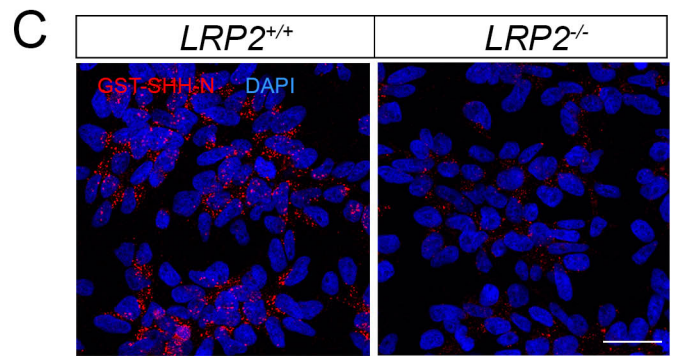
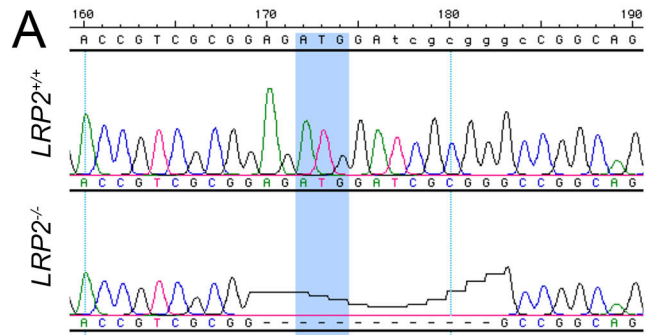


Flemming et al., Figure S1

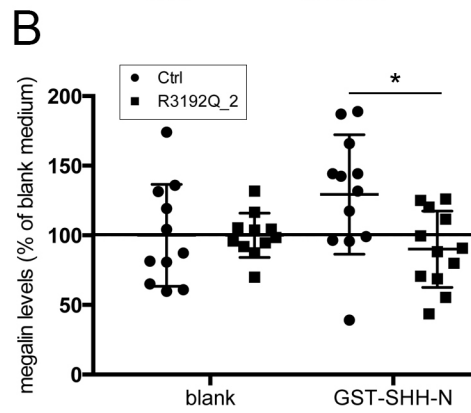
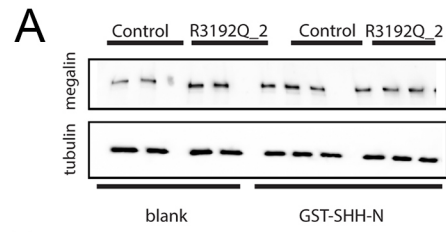




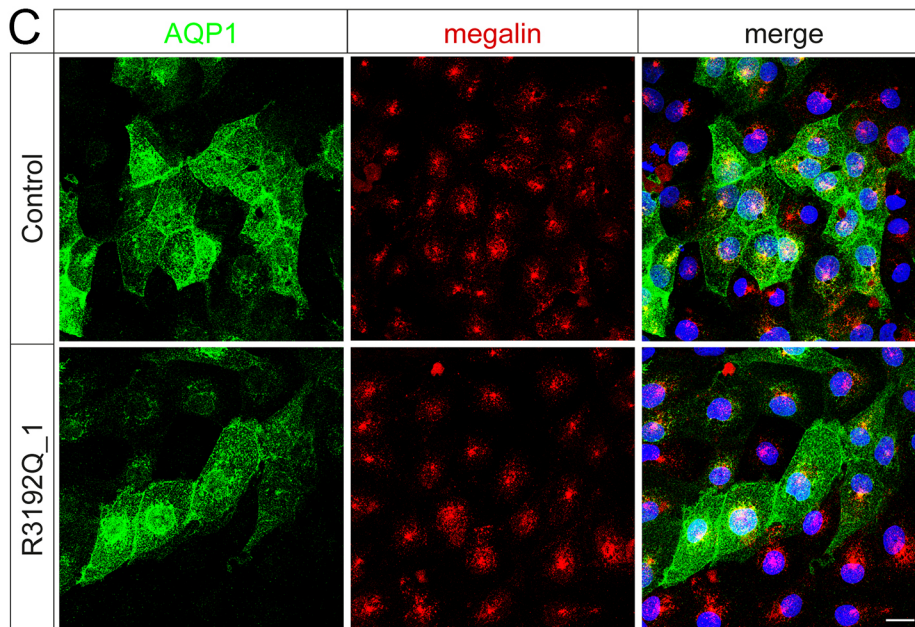
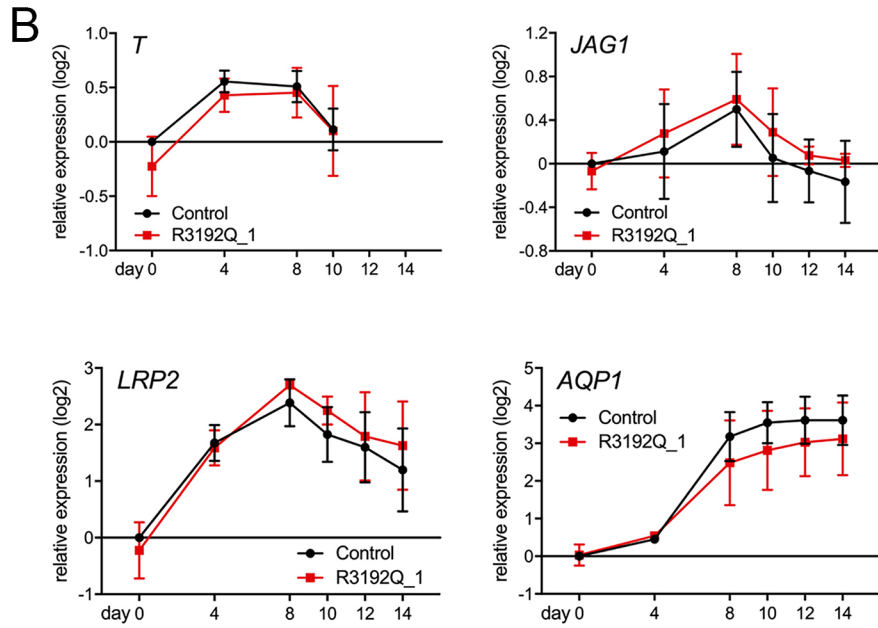
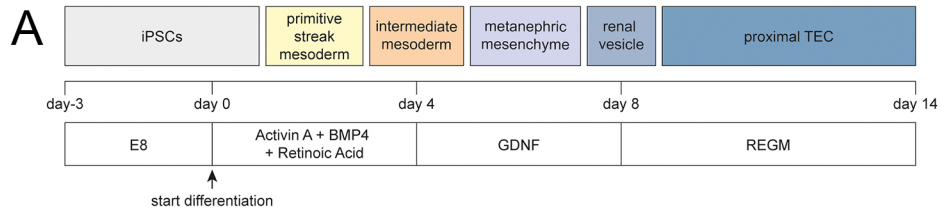




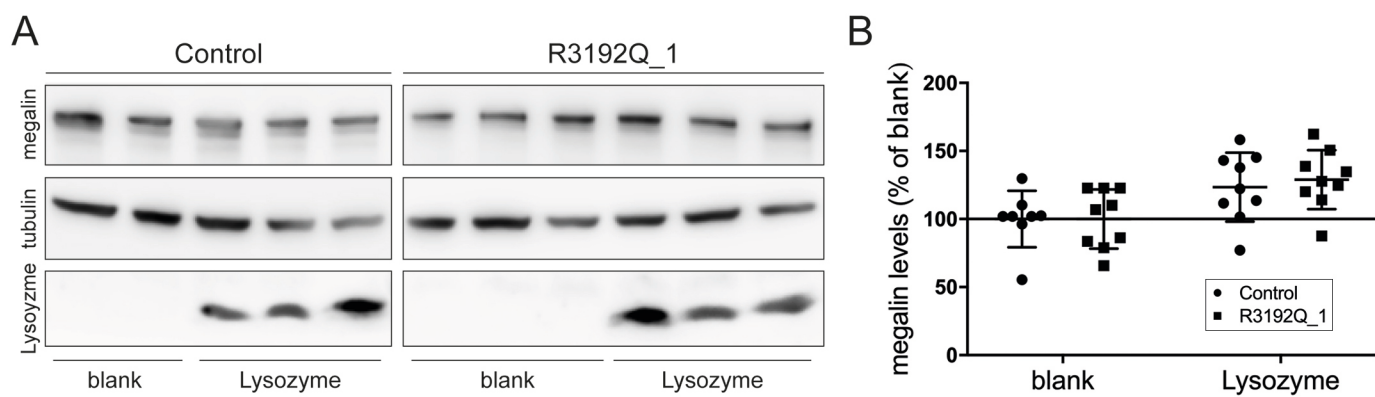
Flemming et al., Figure S5



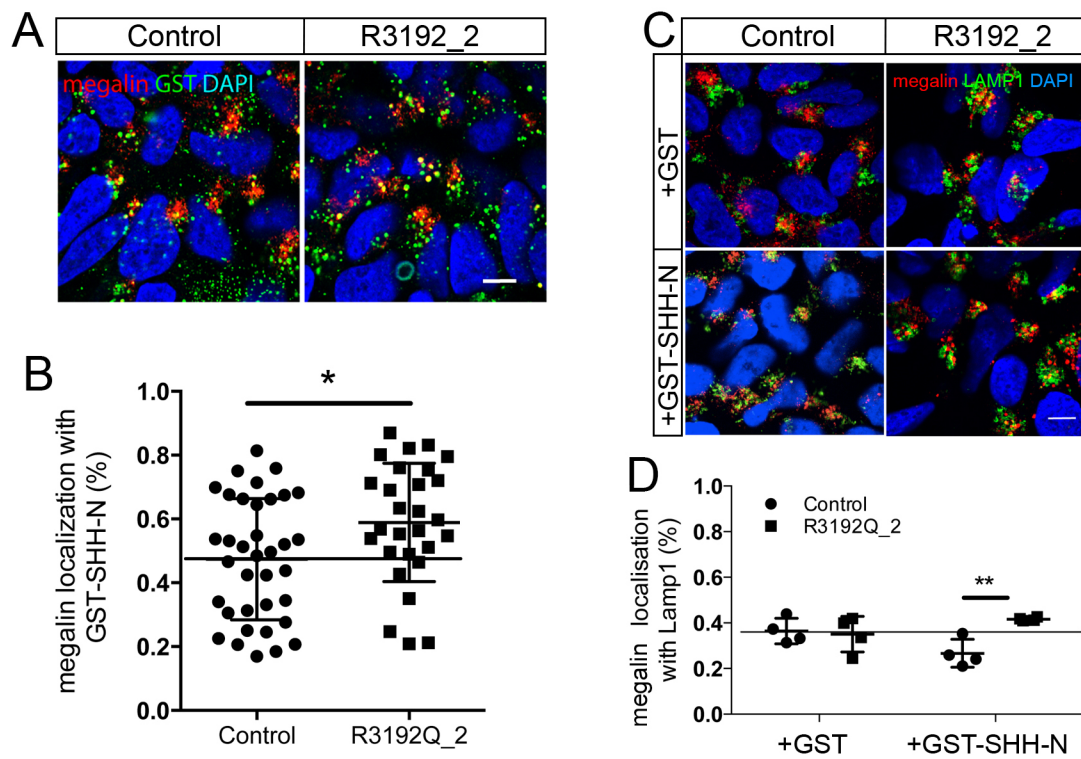
Flemming et al., Figure S6



Flemming et al., Figure S7



Flemming et al., Figure S8



Flemming et al., Figure S9